16. JET-EXIT AND AIRFRAME INTERFERENCE STUDIES ON TWIN-ENGINE-FUSELAGE

AIRCRAFT INSTALLATIONS

By Jack F. Runckel
NASA Langley Research Center

SUMMARY

Jet interference effects on the drag and on the nozzle-afterbody perfor-
mance of twin-engine-fuselage aircraft configured for a Mach number 1.2
mission are discussed. A detailed tailoring of the afterbody with the noz-
zles is required to obtain the best afterbody thrust-minus-drag performance.
Performance improvements were obtained for a model of an aircraft under
development by increasing the afterbody length relative to the jet exits by
the addition of volume between and around the jet exhausts.

INTRODUCTION

In paper no. 15, Corson and Schmeer presented the off-design problems
of isolated nozzles and indicated that sizable nozzle performance penalties
are associated with the installation of the exhaust system in an airplane.
The present paper is concerned with the combined nozzle-afterbody perfor-
mance of twin-engine-fuselage aircraft specifically designed to operate at
a Mach number of 1.2; such aircraft might be required for a high-speed sea-
level dash.

Jet exits on single-engine-fuselage airplanes are usually located at
the end of the afterbody, and jet interference effects are usually confined
to a small region near the jet exhaust. Corson and Schmeer in paper no. 15
referred to several jet-airframe interference studies on single-engine air-
plane models. Twin-engine aircraft can have the jet exits located either at
the terminal section of the fuselage (refs. 1 to 6) or forward on the fuselage
(refs. 7 to 13). In either instance, the arrangement used to provide aft-end
closure of the fuselage ahead of and between the engines determines the mag-
nitude of jet-airframe interference and has an appreciable effect on the con-
figuration drag (refs. 9, 10, and 13 to 15). The jet exhausts can also
affect the airplane stability (refs. 8 to 13), the local loading and skin
temperatures (refs. 7 to 13), and the base pressures (paper no. 15 and
refs. 1 to 3, 6, 8 to 11, and 13).

SYMBOLS

C_p pressure coefficient

D drag

D/q drag coefficient based on unit wing area

d_e diameter of nozzle shroud exit

d_p diameter of primary nozzle

F total gross thrust force

$\dfrac{F - D}{F_i}$ ratio of total gross thrust minus drag aft of separation line to ideal thrust of both primary nozzles

F_i ideal isentropic thrust of both primary nozzles

M free-stream Mach number

$p_{t,j}$ jet total pressure

p_∞ free-stream static pressure

q free-stream dynamic pressure

x distance from primary-nozzle or shroud exit

DISCUSSION

Afterbody Drag

It is known that a large amount of the total drag can occur on the after-body (ref. 16). This situation is particularly serious at transonic speeds where the boattail drag and base drag coefficients are usually maximum (refs. 2, 6, and 17 to 21). Two examples of twin-engine configurations will be discussed to illustrate the magnitude of afterbody drag on this type of aircraft.

A technique for measuring the afterbody drag of aircraft models with jet-power simulation was developed in the Langley 16-foot transonic tunnel (ref. 22). The main features of this system can be examined in figure 1. The photograph shows a research model supported by an underneath sting and a thin strut attached to the forebody to minimize support-system interference. The forebody and wings, which were swept back 108°, provided the correct simulated flow field over the afterbody and propulsion system. The wing tips overlapped but did not touch the afterbody. The model was separated just ahead of the horizontal tails (66-percent-length station) and sealed, and the rear section including the tails

was attached to an internal strain-gage balance. The long engine interfairing was designed to improve the area progression at the rear of the model (refs. 13, 14, and 23).

A powered model of an aircraft under development, which was supported in a similar manner, is shown in figure 2. The wings were swept back 72.5°, and the engine interfairing terminated near the jet exits. Horizontal-tail fairings were located adjacent to both engine nozzles. The separation line was again directly ahead of the horizontal tails at 74 percent of the model length. Force and pressure measurements were obtained on the rear section of the model, with primary and secondary flows in the ejector nozzles and bleed flow at a step exit on the afterbody boattail being controlled variables. Nozzle-afterbody thrust-minus-drag performance will be presented in a subsequent section. It should be noted that the performance ratio used in this paper includes the drag of the afterbody, tails, and nozzle surfaces; therefore, the values of the performance parameter in the present paper are lower than those presented by Corson and Schmeer in paper no. 15.

Both the research and the development models had the inlets faired over. Separate investigations were conducted to determine the effect of fairing over the inlets (ref. 22, for example), and the interference on the afterbody was found to be negligible. The engine exhausts were simulated with hot jets by using the technique described in reference 24.

Comparisons of the afterbody drag of the two configurations (figs. 1 and 2) relative to the drag coefficient of the complete models are presented in figure 3 for a Mach number of 1.2 at sea level and adjusted for full-scale Reynolds numbers. The afterbody of the research model, shown crosshatched, comprised about one-third of the the body length and contained about 36 percent of the total wetted area. The bar next to this model represents the drag coefficient of the entire configuration based on unit area. With the jets operating at a typical turbofan pressure ratio at a Mach number of 1.2, the afterbody drag was 41 percent of the total drag.

The afterbody of the development model comprised only one-fourth of the complete model length but had about 39 percent of the total wetted area. The afterbody drag, for the same operating conditions, was 46 percent of the complete model drag. These results show that a large percentage of the total drag occurs on a relatively small portion of the afterbody of twin-engine aircraft configurations.

Afterbody Closure

Several areas on twin-engine-fuselage airplanes are known to be sensitive to jet interference effects. Among these are the afterbody boattail (refs. 9 and 13), tail surfaces (refs. 10 and 11), and fuselage bases (refs. 2, 5, 6, and 10). Inasmuch as the afterbody of an aircraft may be a region of high local drag, an examination of the afterbody of a twin-engine aircraft was made to determine whether detailed tailoring would render better performance. A basic difference in the two configurations of figures 1 and 2 is the way the body

between the engine nozzles is designed. This terminal section is called the engine interfairing.

Pressure distributions on the interfairings of the two configurations are shown in figure 4. The nozzle exits, indicated by the diameter d_e, are located at the reference station 0 on the abscissa. The axial distance x from the exit is given in exit diameters. Pressure measurements are shown for the row of orifices closest to the center line of the exhaust nozzles.

The research model had a long interfairing extending downstream of the jet exits. The results obtained with the jets off indicate a gradual pressure recovery from low pressures near the engine base region. With the jets on, the interference was generally favorable, increasing the pressures to a positive value and causing thrust on part of the interfairing (ref. 22).

The wedge-shape interfairing on the development model was mostly ahead of the jet exit station. The interfairing pressures of this model were lower than those of the research model with the jets off. Jet operation produced a relatively small increase in pressure, an indication that the region between the engines remains an effective base drag area.

These results prompted an investigation of the flow field behind the aft end of the development model. An axial static probe was extended downstream of the model along the center line to measure pressures behind the model. The results are given in figure 5. The pressures obtained with the jets both off and on again show low pressures on the interfairing; however, an abrupt rise which occurred in pressure directly behind the model indicates that extending the fuselage volume into this greater-than-free-stream pressure field would probably reduce afterbody drag.

Engine-Interfairing Studies

Past work has shown that configurations with jets exhausting alongside aft-sloping fuselage surfaces have had favorable jet interference effects on drag; that is, jet operation increased the local pressures in the regions adjacent to and downstream of the jet exits (paper no. 15 and refs. 8 to 13). Usually, excess low-energy internal air is available near the nozzle, and this dumped air can provide a cooling film between the hot exhaust and the fuselage skin (refs. 5 and 10). The results of reference 15 indicate that axial-force reduction by interference between a jet and a neighboring afterbody would be large at supersonic speeds. In addition, an extension of the interfairing would improve the area progression (refs. 4, 14, and 23) and probably would reduce the wave drag.

The rest of this paper will be concerned with only the development model, and the discussion will be confined to performance at a Mach number of 1.2. The first attempt to improve the afterbody performance involved an increase in interfairing length and a volume addition, as is shown in figure 6. A blow-in-door nozzle which had the doors closed next to the interfairing and tail fairings was utilized to allow for maximum volume between the nozzles. The

nozzle-afterbody performance parameter $\dfrac{F - D}{F_i}$ is the ratio of the total gross thrust minus the drag aft of the line of separation to the ideal thrust of the two primary nozzles. This ratio includes changes in both nozzle performance and afterbody drag due to interfairing differences and jet interference effects. The performance of the two configurations is plotted as a function of jet pressure ratio for identical internal and external flow conditions. These and all subsequent data are presented for zero secondary airflow and a corrected bleed-flow ratio of about 8 percent.

The gain in performance for the configuration with the extended interfairing is about 5 percent. This performance gain is equivalent to about a 30-count decrease in drag coefficient for the airplane model. It is apparent that major gains in performance are possible by working on the nozzle-afterbody region of twin-engine-fuselage aircraft.

The initial improvement in performance obtained with an extended interfairing led to further work to explore this concept. An investigation was conducted to determine the effect of engine interfairing and aft-end changes on the performance of the model with a short, small-diameter nozzle shroud. The results are presented in figure 7. Incremental nozzle-afterbody performance gains are plotted as a function of interfairing length in primary-nozzle diameters. The primary-nozzle diameter was constant for these and subsequent data and corresponded to the scaled nozzle area required for the 1.2 Mach number sea-level dash. The jet pressure ratio was about 3.4 for all configurations. Shown in figure 7 are interfairings of short (① and ⑥), medium (② and ④), and long (③ and ⑤) extensions.

The interfairing-length differences are shown in the photographs in figure 8. The basic short interfairing is shown in the picture on the left, the medium extension of the interfairing is presented in the center photograph, and the long interfairing is shown on the right. The performance of these configurations (fig. 7), indicated by numbers ① , ② , and ③ , respectively, shows that a medium extension of the interfairing (configuration ②) produced a performance gain of over 2 percent. A further increase in length to the long interfairing (configuration ③) gave an additional gain of 1 percent. The increase in performance with increasing interfairing length indicates that adding length downstream of the jet exits can provide performance improvements due to better closure, a more favorable flow field, and more favorable jet interference effects.

The numbers ④ and ⑤ in figure 7 represent configurations having the same medium and long interfairings as those indicated by the numbers ② and ③ , respectively. The differences in these configurations are shown in the photographs in figure 9. Additional volume was added around the nozzles by installing larger tail fairings which house the horizontal-tail mechanism. The small tail fairings on the medium- and long-interfairing configurations are shown in the bottom pictures and the large tail fairings on the same configurations are shown in the photographs at the top.

The larger tail fairings provided further substantial increases in performance, as shown by the data points for configurations ④ and ⑤ in figure 7.

The use of tail fairings to reduce transonic drag through favorable jet inter-
ference and application of the area rule are discussed in reference 14.

A different approach was also tried by using a concave-base interfairing
concept based on the concave-base plug nozzle (ref. 25). Figure 10 shows the
concave-base interfairing concept. The long interfairing shown on the left was
cut-off at about the same length as the basic interfairing (right photograph),
and the base was recessed, as shown in the center (configuration ⑥). The cut-
off interfairing is essentially a volume addition relative to the basic inter-
fairing since it brings the interfairing surfaces closer to the jet exits. The
performance of this configuration, shown by the number ⑥ in figure 7, was
equal to that of the model with the long interfairing (configuration ③).
Although the cut-off configuration was about the same length as the basic con-
figuration, the pressure coefficients on the sides and base of the concave-base
interfairing (configuration ⑥) were higher than those of the wedge-shape inter-
fairing (configuration ①) and, therefore, the effective base drag of the cut-
off configuration was lower.

The results presented in figure 7 indicate that adding length to and/or
volume between the short, small-diameter nozzles provided performance improve-
ments relative to the model with the basic interfairing. The main benefits are
believed to be caused by more favorable jet interference effects and lower
slopes on the afterbody between the engines for the altered configurations. Of
course, there are compensating problems, such as weight and balance, added skin
friction, and high local skin temperatures, which must be considered in making
aft-end changes.

Nozzle-Afterbody Integration

Other work on nozzle sizing indicated that nozzles having larger diameters
than those previously discussed would provide better performance. Models
designed to integrate a large-diameter shroud with a long interfairing were
investigated and the results are compared in figure 11. The performance and
length parameters are the same as those of figure 7. The reference level of
performance is again that of the short, small-diameter nozzle with the basic
interfairing, indicated by the solid circle (configuration ①). The open sym-
bols represent the large-diameter shrouds. The squares represent configurations
with long, large-diameter nozzles, such as those shown in figure 2.

Some of the large-diameter nozzle-afterbody combinations are shown in fig-
ure 12. The long nozzle with the basic interfairing is shown in the left pic-
ture. This configuration had almost 2-percent better performance than the ref-
erence nozzle, as indicated by the square directly above the solid symbol in
figure 11.

The addition of a long interfairing to the long nozzle (square symbol at
$x/d_p = 3.25$) provided a gain in performance of about 1 percent. Shortening the
nozzle with the same long interfairing provided an additional gain, as indicated
by the diamond-shape symbol. This configuration is shown in the center photo-
graph of figure 12. These results are consistent with those shown in figure 7

since shortening the nozzle with the same length interfairing exposes a greater portion of the interfairing to favorable jet interference effects.

The terminal-fairing nozzle shown in the right photograph in figure 12 represents a more complete integration of the nozzle with the afterbody. This concept (ref. 26) has been discussed by Corson and Schneer in paper no. 15. The terminal-fairing nozzle maintained the diameters and blow-in-door features of the large nozzle, but had a short, fixed shroud. A photograph of the terminal-fairing nozzle configuration is presented on the right-hand side of figure 12. This nozzle-afterbody combination had a large-volume interfairing and utilized the interfairing (refs. 27 and 28) and tail fairing (ref. 14) as part of the nozzle surface. The nozzle had eight terminal bodies, and the open spaces between the terminal fairings allowed ventilation between the jet and the free stream.

The performance of the terminal-fairing configuration is shown by the triangle-shape symbol in figure 11. This combination produced the highest nozzle-afterbody performance at Mach 1.2 of the large-shroud-nozzle—afterbody models investigated. The data presented by Corson and Schmeer in paper no. 15 and the results of reference 15, which indicate favorable jet interference effects at supersonic speeds, indicate that the supersonic performance of this configuration would also be good. (See ref. 27.)

CONCLUDING REMARKS

The results presented indicate that a relatively large amount of the total drag, of the order of 40 to 50 percent, occurs on the aft end of twin-engine-fuselage aircraft at transonic speeds. The performance of configurations with jet exits at the rear of the afterbody may be improved by increasing the after-body length relative to the jet exits by the addition of volume between and around the jet exhausts. A detailed tailoring of the afterbody with the nozzles is required to obtain the best afterbody thrust-minus-drag performance. Of course, there are compensating problems, such as weight and balance, added skin friction, and high local skin temperatures, which must be considered in making aft-end changes. The cutoff large-volume interfairing represents a possible compromise.

REFERENCES

1. Salmi, Reino J.; and Klann, John L.: Investigation of Boattail and Base
   Pressures of Twin-Jet Afterbodies at Mach Number 1.91. NACA RM E55C01,
   1955.

2. Leiss, Abraham: Free-Flight Investigation of Effects of Simulated Sonic
   Turbojet Exhaust on the Drag of Twin-Jet Boattail Bodies at Transonic
   Speeds. NACA RM L56D30, 1956.

3. Rustemeyer, A. H.; and Twomey, E. J.: Thrust and Drag Characteristics of
   Several Turbojet Exhaust Models at Supersonic and High-Subsonic Mach Num-
   bers. R-0922-16 (Contract NOa(s)55-134-c), Res. Dept., United Aircraft
   Corp., June 1957.

4. Reyn, J. W.: On the Optimum Body Shape at the Base With an Application to
   a Fuselage With Jet Engine Tail Pipes at Transonic Speeds. Rept. VTH-101,
   Tech. Hogeschool Delft Vliegtuigbouwkunde, Nov. 1958.

5. Bottorff, Marion R.: Wind Tunnel Tests at Mach Numbers From .82 to 2.05 of
   a 4.2% Scale A3J-1 Base Drag Model Using Hydrogen-Air Combustors for Jet
   Simulation. USCEC Rept. 65-7, Aerodyn. Test Lab., NMC, Univ. of Southern
   California, Nov. 2, 1959.

6. Langfelder, Helmut: Low-Drag Installation of Twin Propulsion Nozzles in the
   Rear of the Fuselage for Transonic and Supersonic Flight. Aerodynamics of
   Power Plant Installation, Pt. I, AGARDograph 103, Oct. 1965, pp. 195-216.

7. Swihart, John M.; and Crabill, Norman L.: Steady Loads Due to Jet Inter-
   ference on Wings, Tails, and Fuselages at Transonic Speeds. NACA RM L57D24b,
   1957.

8. Mitcham, Grady L.: A Summary of the Longitudinal and Lateral Stability and
   Control Characteristics Obtained From Rocket-Model Tests of a Swept-Wing
   Fighter-Type Airplane at Mach Numbers From 0.5 to 1.9. NACA RM L56K19,
   1957.

9. Lee, Edwin E., Jr.; and Salters, Leland B., Jr.: Effects of Afterbody
   Shape and Hot Jet Exhausts on Pressures, Temperatures, and Drag of a Twin-
   Engine Fighter-Airplane Model Having an Overhanging Fuselage. NASA MEMO
   12-29-58L, 1959.

10. Lee, Edwin E., Jr.; Foss, Willard E., Jr.; and Runckel, Jack F.: Jet Effects
    on the Base, Afterbody, and Tail Regions of a Twin-Engine Airplane Model
    With High and Low Horizontal-Tail Locations. NASA TM X-2, 1959.

11. Lee, Edwin E., Jr.; and Mercer, Charles E.: Jet Interference Effects on a
    Twin-Engine Attack-Type-Airplane Model With Large Speed-Brake, Thrust-
    Spoiler Surfaces. NASA TM X-454, 1961.

12. Mercer, Charles E.; Salters, Leland B., Jr.; and Capone, Francis J.: After-body Temperatures, Pressures, and Aerodynamic Characteristics Resulting From Extension of Speed-Brake Configurations Into the Exhaust Jets of a Twin-Engine Attack-Type-Airplane Model. NASA TM X-517, 1961.

13. Foss, Willard E., Jr.; Runckel, Jack F.; and Lee, Edwin E., Jr.: Effects of Boattail Area Contouring and Simulated Turbojet Exhaust on the Loading and Fuselage-Tail Component Drag of a Twin-Engine Fighter-Type Airplane Model. NACA RM L58C04, 1958.

14. Ballinger, J. G.; and Horn, R. C.: Final Report - Afterbody Drag Reduction by Application of the Area Rule Accounting for Jet Exhaust. WADC Tech. Rept. 57-634, ASTIA Doc. No. AD 142335, U.S. Air Force, Dec. 1957.

15. Pitts, William C.; and Wiggins, Lyle E.: Axial-Force Reduction by Inter-ference Between Jet and Neighboring Afterbody. NASA TN D-332, 1960.

16. Stoney, William E., Jr.: Some Experimental Effects of Afterbody Shape on the Zero-Lift Drag of Bodies for Mach Numbers Between 0.8 and 1.3. NACA RM L53I01, 1953.

17. Henry, Beverly Z., Jr.; and Cahn, Maurice S.: Additional Results of an Investigation at Transonic Speeds To Determine the Effects of a Heated Propulsive Jet on the Drag Characteristics of a Series of Related After-bodies. NACA RM L56G12, 1956.

18. Cubbage, James M., Jr.: Jet Effects on the Drag of Conical Afterbodies for Mach Numbers of 0.6 to 1.28. NACA RM L57B21, 1957.

19. Hargis, Calvin B., Jr.; Davison, P. H.; and Savage, S. B.: Methods for Estimating Base Pressures on Aircraft Configurations. WADC Tech. Note 57-28, ASTIA Doc. No. AD 110742, U.S. Air Force, July 1957.

20. Swihart, John M.; and Nelson, William J.: Performance of Multiple Jet-Exit Installations. NACA RM L58E01, 1958.

21. Cubbage, James M., Jr.: Effect of Multiple-Jet Exits on the Base Pressure of a Simple Wing-Body Combination at Mach Numbers of 0.6 to 1.27. NASA TM X-25, 1959.

22. Runckel, Jack F.; Lee, Edwin E., Jr.; and Simonson, Albert J.: Sting and Jet Interference Effects on the Afterbody Drag of a Twin-Engine Variable-Sweep Fighter Model at Transonic Speeds. NASA TM X-755, 1963.

23. Bielat, Ralph P.; Robins, A. Warner; and Alford, William J., Jr.: The Transonic Aerodynamic Characteristics of Two Variable-Sweep Airplane Con-figurations Capable of Low-Level Supersonic Attack. NASA TM X-304, 1960.

24. Runckel, Jack F.; and Swihart, John M.: A Hydrogen Peroxide Hot-Jet Sim-ulator for Wind-Tunnel Tests of Turbojet-Exit Models. NASA MEMO 1-10-59L, 1959.

25. Corson, Blake W., Jr.; and Mercer, Charles E.: Transonic Thrust and Drag Characteristics of an Annular Nozzle Having a Semitoroidal Concave Plug. NASA TM X-958, 1964.

26. Runckel, Jack F.: Preliminary Transonic Performance Results for Solid and Slotted Turbojet Nacelle Afterbodies Incorporating Fixed Divergent Jet Nozzles Designed for Supersonic Operation. NASA MEMO 10-24-58L, 1958.

27. Weir, John: Aircraft Performance Problems Associated With Engine and Intake Installation. Aerodynamics of Power Plant Installation, Pt. I, AGARDograph 103, Oct. 1965, pp. 173-194.

28. Connors, James F.; and Meyer, Rudolph C.: Investigation of an Asymmetric "Penshape" Exit Having Circular Projections and Discharging Into Quiescent Air. NACA RM E56K09a, 1957.

RESEARCH MODEL
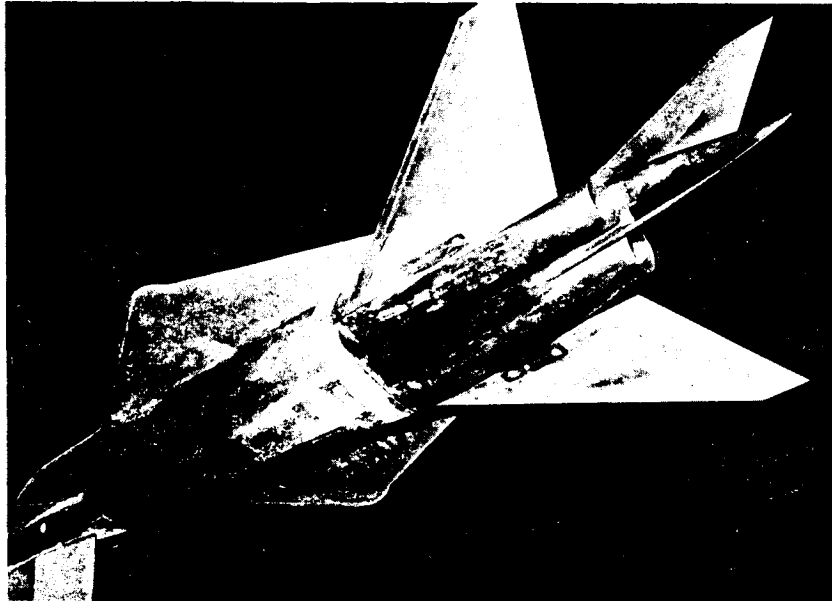
Figure 1   L-2681-1

DEVELOPMENT MODEL
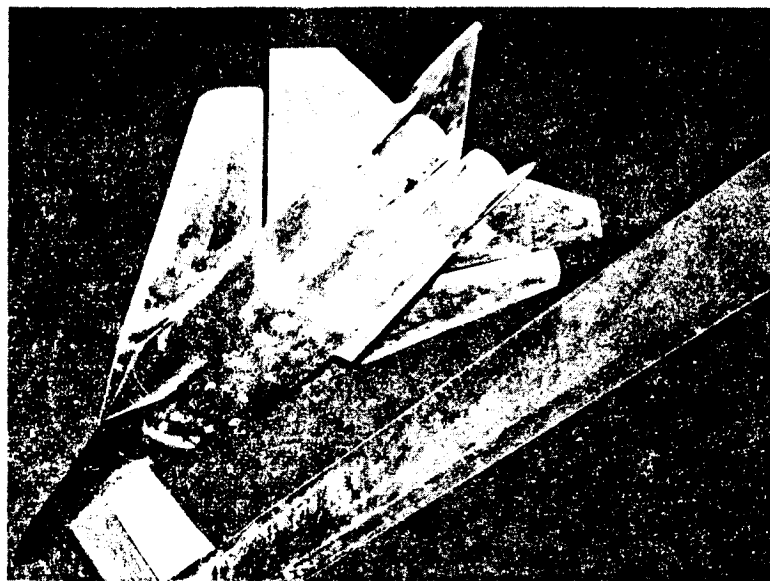
Figure 2   L-2681-2

COMPARISON OF TOTAL AND AFT-END DRAG
M = 1.2 AT SEA LEVEL

RESEARCH MODEL

PERCENT
D/q

100

41

0

DEVELOPMENT MODEL

PERCENT
D/q

100

46

0
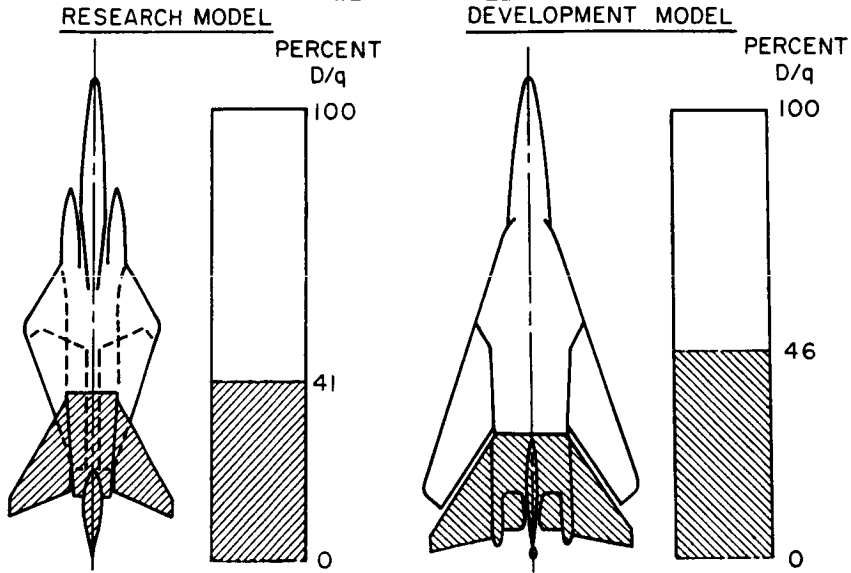
Figure 3

ENGINE INTERFAIRING PRESSURE DISTRIBUTIONS
M = 1.2

RESEARCH MODEL

DEVELOPMENT MODEL

d_e

x

$-x$

d_e

JETS
○ OFF
□ ON

.2

C_p

0

-.2

-.4

0   1   2   3

-2   -1   0

DISTANCE FROM NOZZLE EXIT, x/d_e
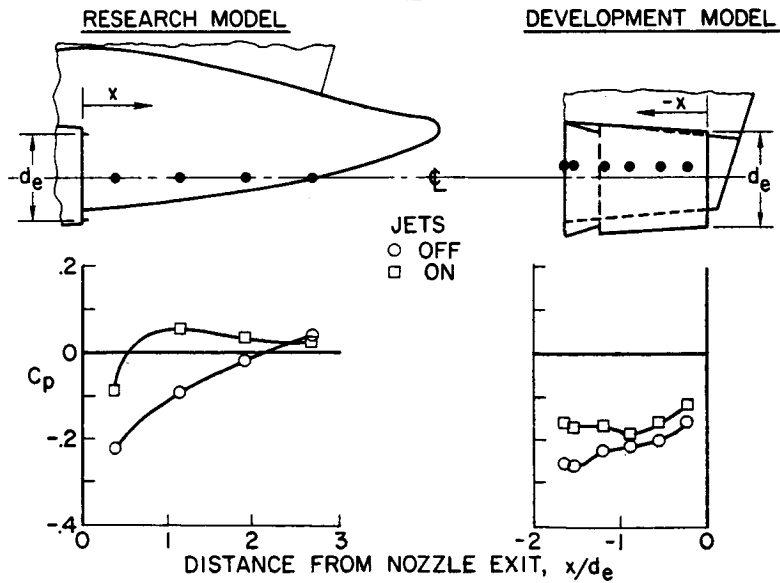
Figure 4

FLOW-FIELD STATIC-PRESSURE DISTRIBUTIONS
M = 1.2
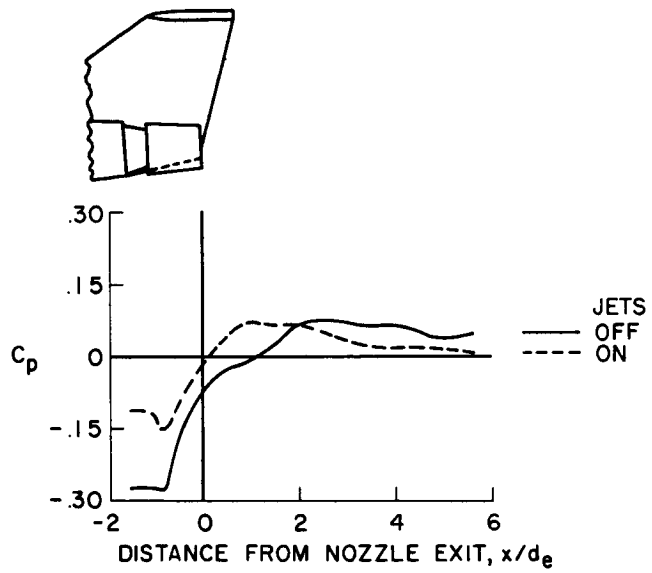
Figure 5

PERFORMANCE OF
BASIC- AND EXTENDED-INTERFAIRING CONFIGURATIONS
M = 1.2
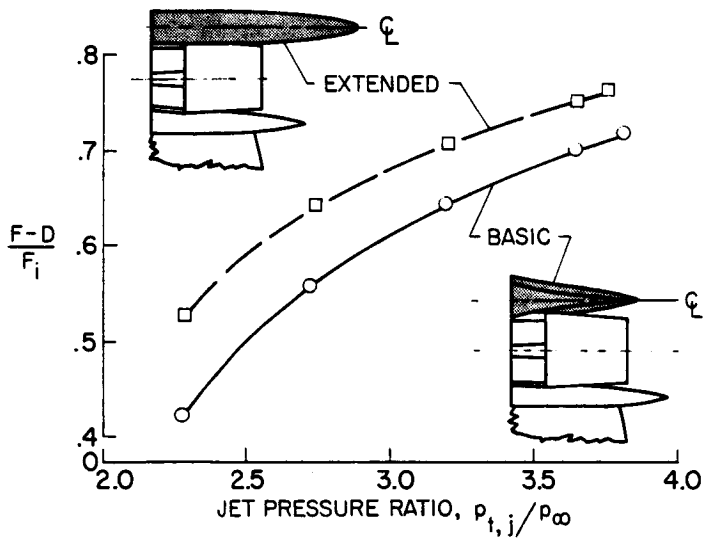
Figure 6

EFFECT OF AFTERBODY LENGTH AND VOLUME
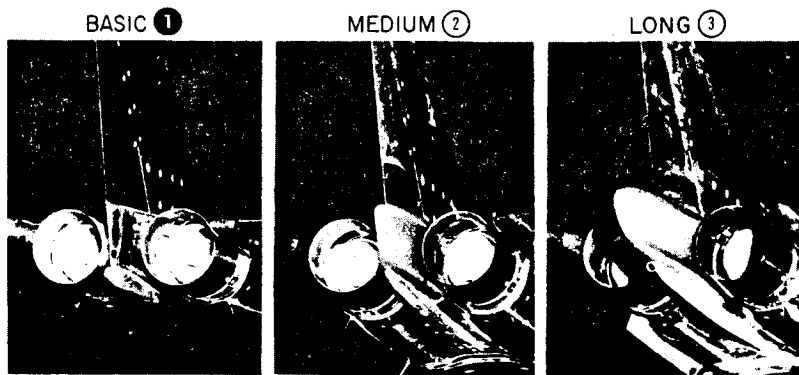### M=1.2; SHORT SMALL-DIAMETER NOZZLE SHROUD

PERFORMANCE INCREMENT, $\Delta\left(\dfrac{F-D}{F_i}\right)$, PERCENT

INTERFAIRING LENGTH FROM PRIMARY NOZZLE, x/d_p
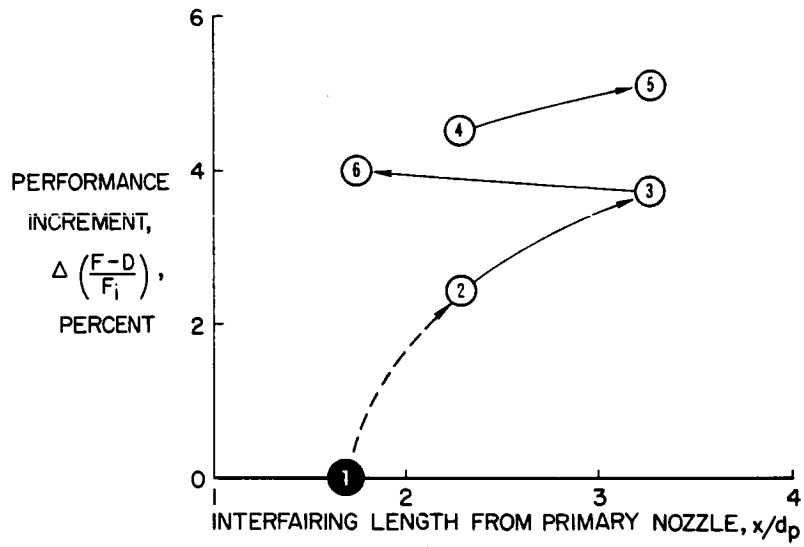
Figure 7

INTERFAIRING EXTENSIONS

BASIC ❶   MEDIUM ②   LONG ③

Figure 8

L-2681-8

242

TAIL FAIRINGS

LARGE

MEDIUM INTERFAIRING ④

LONG INTERFAIRING ⑤

SMALL

MEDIUM INTERFAIRING ②
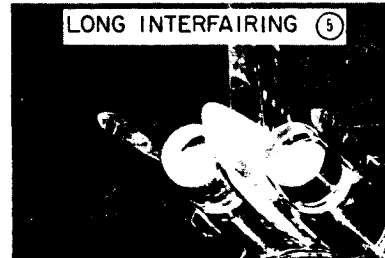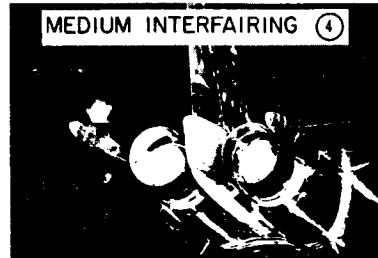
LONG INTERFAIRING ③

Figure 9   L-2681-9
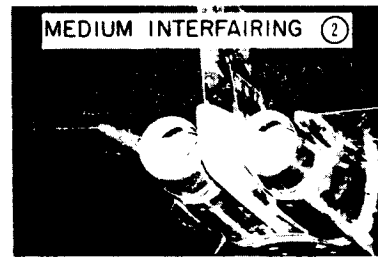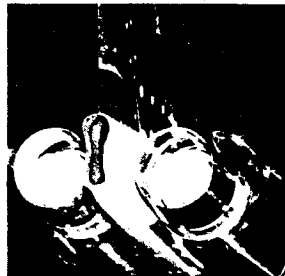
INTERFAIRINGS

LONG ③   CUT-OFF ⑥   BASIC ❶
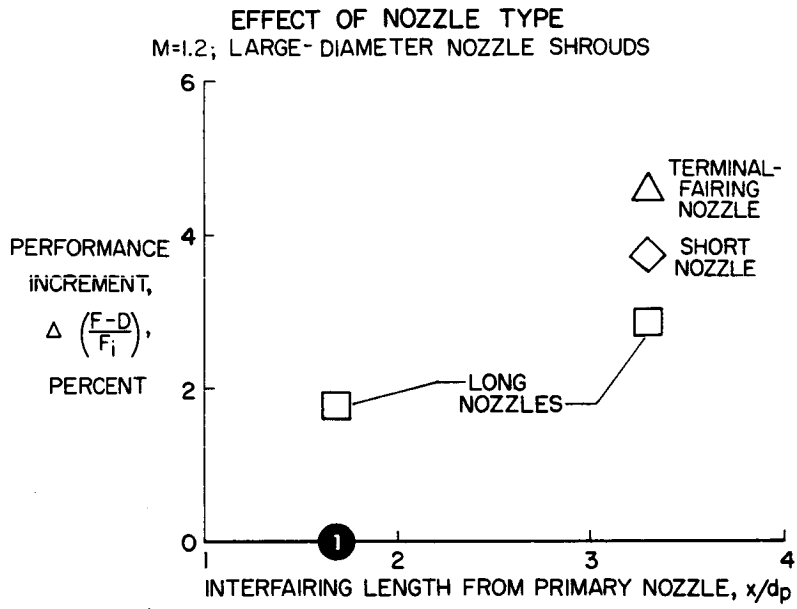
Figure 10   L-2681-10

EFFECT OF NOZZLE TYPE
M=1.2; LARGE-DIAMETER NOZZLE SHROUDS

PERFORMANCE
INCREMENT,

$\Delta \left(\dfrac{F-D}{F_i}\right)$,

PERCENT

TERMINAL-
FAIRING
NOZZLE

SHORT
NOZZLE

LONG
NOZZLES

INTERFAIRING LENGTH FROM PRIMARY NOZZLE, x/d_p
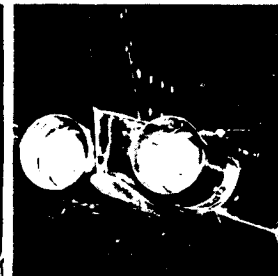
Figure 11

LARGE-DIAMETER NOZZLE SHROUDS

LONG □   SHORT ◇   TERMINAL FAIRING △

BASIC
INTERFAIRING

LONG
INTERFAIRING

LONG
INTERFAIRING

Figure 12   L-2681-12

244